OBTAINING THE MAXIMUM PRESSURE ANGLE IN TRANSLATING RADIAL CAM-FOLLOWER

José Maria Bezerra Silva, zemaria@ufpe.br
Félix Christian G. Santos, fcgs@ufpe.br
José Maria Andrade Barbosa, jmab@ufpe.br
Departamento de Engenharia Mecânica da Universidade Federal de Pernambuco, Centro de Tecnologia e Geociências, Rua Acadêmico Hélio Ramos S/N, Cidade Universitária, Recife-PE.

Abstract. *In the classical cam displacement diagrams, e.g. skewed parabolic motion, simple or double-dwell harmonic motion, cycloidal motion or the cubic motion, the cam pressure angle in a rise or fall segment is often a function of two variables, that is, the cam rotation angle and the cam prime circle radius. Consequently this will hamper us to obtaining the maximum pressure angle, since we have only one equation and two unknown variables, but being a decreasing function with respect to the prime circle radius. On the other hand the prime circle radius will determine the cam size and consequently should be obtained as a function of a maximum pressure angle. Some authors have proposed a graphical nomogram for this computation, with some limitations and inaccuracy. This work proposes a new way to calculate the prime circle radius analytically, based on some trigonometric expressions.*

Keywords: *cams, mechanisms, machines*

1. INTRODUCTION

In general, in the design of cams with radial translating followers, the performance and efficiency are closely linked to the maximum pressure angle, so that initially one determines the maximum pressure angle such that friction and vibration on the follower are reduced to tolerable levels. From that the problem is to determine a cam-follower geometry, which is as compact as possible in order to have a good dynamic response and to reduce the mechanical power due to a lower inertia, Koomok and Muffley (1955).

In this sense, the prime circle radius, R_p, reflects the most important determinant factor on the cam size Yu and Lee (1998). Furthermore the value of the prime circle radius for each cam curve type is directly proportional to the cam size and inversely proportional to the value of the maximum pressure angle. Thus, there will be an unique value for R_p that will satisfy the given maximum pressure angle. A value smaller than that, which might be interesting for the cam geometry and efficiency, will result in a maximum pressure angle larger than the specified one. On the other hand a larger value, while improving the angle of pressure to lower, will result in higher power demand and excess of material and, thus, resulting into additional costs.

According to the above, the problem is to determine, with a desired accuracy, the prime circle radius from a given maximum pressure angle. Unfortunately, the expressions developed so far do not allow analytical computation of R_p. Calculation processes presented by several authors, who have approached the subject, are based on nomograms, iterative numerical methods or by pure and simple computer trial and error Rothbart (2004), Uicker *et al.* (2010), Norton (2009).

In this work the analytical expressions for calculating the prime circle radius are obtained, starting from the premise that one does not need the rise angle of the follower, θ_0, where the maximum pressure angle is reached.

2. NOTATION

φ	pressure angle
$\hat{\varphi}$	maximum pressure angle
β	elevation angle
β_a	elevation angle to the first parabolic segment (parabolic curve only)
β_b	elevation angle to the second parabolic segment (parabolic curve only)
θ	cam angle, ranging from 0 to β on elevation diagrams
θ_0	critical value, where occurs the maximum pressure angle
R_p	prime circle radius
h	maximum displacement of follower
ε	offset of the follower

all angles in degrees

3. PRELIMINARY CONSIDERATIONS

According to Rothbart (2004), in radial cams with a translating roller follower the pressure angle φ is defined as the angle between the direction of follower movement with the direction of the axis of transmission. The axis of transmission, Figure 1, is normal to cam primitive curve passing through the centre of the roller. The pitch curve is obtained from an offset on the cam profile, equal to the radius of the roller. Note that an angle φ of $\frac{\pi}{2}$ makes the movement of the follower impossible, while with $\varphi = 0$ the cam does not move the follower Gonzales-Palacios and Angeles (1993).

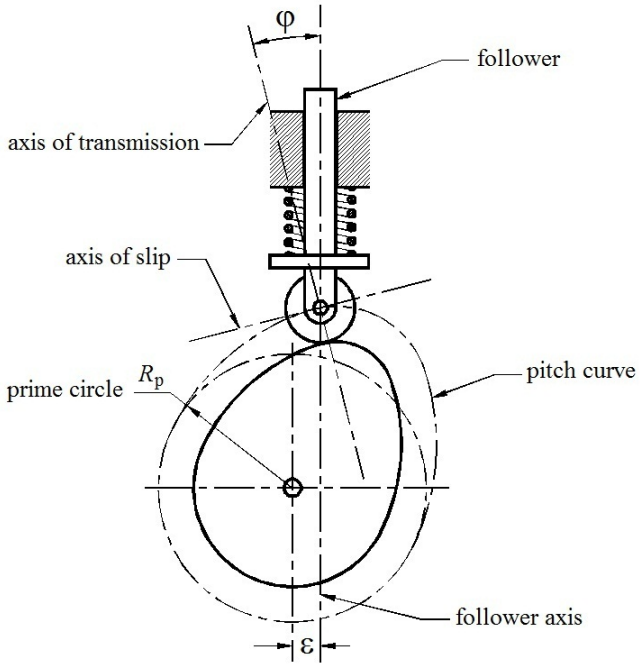

Figure 1. Prime circle, pitch curve and pressure angle for a radial cam with translating follower

During a radial follower elevation, the pressure angle varies from 0 to $\hat{\varphi}$ and goes back to zero again. Geometric relations, Figure 1 and the cam angular velocity can be used to obtain the following expression for the tangent of φ as a function of the rotation angle, θ (ranging from zero to β) and R_p:

$$\tan\varphi = \frac{f'(\theta) - \varepsilon}{f(\theta) + \sqrt{R_p^2 - \varepsilon^2}} \tag{1}$$

where (ε) is the follower's offset. Note that $\tan\varphi$ is a surface depending on θ and R_p, being a strictly decreasing function of R_p. So, given a specific value for φ, means that a plane will cut that surface, defining a curve on (θ, R_p). Now, one may require that the derivative of $\tan\varphi$ with respect to θ is equal to zero, in order to find an stationary value. That will result in a differential equation, which is a condition for θ_0. This is then solved, obtaining $theta_0$ as a function of R_p, which is another curve on (θ, R_p). The intersection of those curves define an unique point (θ_0, R_p), which is the desired solution. This procedure is described below. Differentiating Eq. (1) and setting it to zero result in:

$$f''(\theta_0)\Big[f(\theta_0) + \sqrt{R_p^2 - \varepsilon^2}\,\Big] - f'(\theta_0)\Big[f'(\theta_0) - \varepsilon\Big] = 0 \tag{2}$$

where $\hat{\varphi}$ is the angle φ obtained by the introduction of the argument θ_0 in Eq. (1). Isolating the term $\sqrt{R_p^2 - \varepsilon^2}$ in Eq. (1) and inserting it in Eq. (2), we get:

$$\tan\hat{\varphi} = \frac{f''(\theta_0)}{f'(\theta_0)} \tag{3}$$

Afterwards we'll comment on followers with $\varepsilon \neq 0$. For the moment we will consider the $\varepsilon = 0$, a situation more common in flat cams. In this case Eq. (1) becomes:

$$\tan\varphi = \frac{f'(\theta)}{f(\theta) + R_p} \tag{4}$$

and

$$f''(\theta_0)(f(\theta_0) + R_p) - f'(\theta_0)^2 = 0 \tag{5}$$

Note that Eq. (3) is independent of ε, and can be used in both cases. Eq. (3) will be important in obtaining the equations for offset followers, implying that we should only repeat the calculations from Eq. (2), taking advantage of all previous developments.

4. CALCULATION OF THE PRIME CIRCLE

As it was mentioned before, now the problem is to obtain the prime circle radius from a known $\hat{\varphi}$. For that we use Eq. (4) and Eq. (5) in order to compute variables, θ_0 and R_p. Since the function $f(\theta)$ is usually a composition of trigonometric functions, solutions to Eq. (4) will often be transcendental expressions and thus difficult to obtain.

Uicker *et al.* (2010) Proposed a nomogram, Figure 2, which allows the calculation of R_p for the simple harmonic motion and for cycloidal motion. Norton (2009) suggests an initial estimate for R_p and a subsequent iteration, which provide an approximate solution.

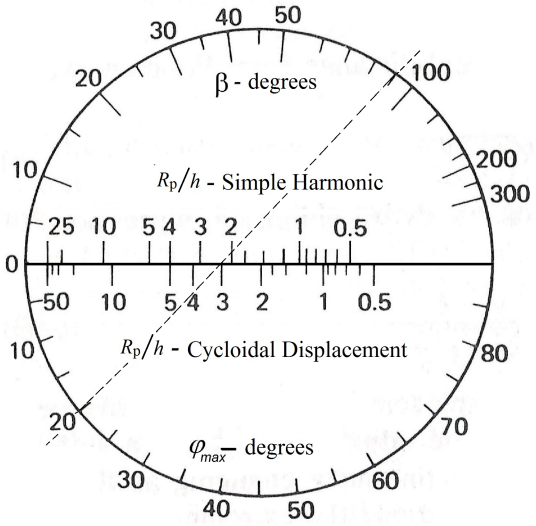

Figure 2. Nomogram showing that for $\hat{\varphi} = 20^o$ and $\beta = 90^o$ the solution is $\frac{R_p}{h} = 2.3$ for the harmonic motion and $\frac{R_p}{h} = 3.1$ for the cycloidal motion

Our approach on calculating the prime circle radius will consider the elevation curves of type parabolic, simple harmonic, double harmonic and cycloidal, because these curves involve transcendental functions that make it difficult to obtain the maximum pressure angle φ.

On the other hand offset followers are of interest only when a reduction in the transmission angle is desired. In this case the offset will provide the desired improvement. Thus the analysis is always made with the radial follower, that is $\varepsilon = 0$, which will be the object of most of our development. Therefore the equations (3), (4) and (5) will be key to obtaining the prime circle radius as a function of $\tan\hat{\varphi}$.

4.1 Calculation of R_p for the Parabolic Motion

As it is shown in Figure 3, the parabolic curve motion consists of two sections of parabolic functions. So the expressions take the form:

$$f(\theta) = \begin{cases} \frac{h}{\beta\beta_a}\theta^2 & \text{if } 0 \le \theta \le \beta_a \\ h - \frac{h}{\beta\beta_b}(\beta - \theta)^2 & \text{if } \beta_a < \theta \le \beta \end{cases} \tag{6}$$

$$f'(\theta) = \begin{cases} \frac{2h}{\beta\beta_a}\theta & \text{if } 0 \le \theta \le \beta_a \\ \frac{2h}{\beta\beta_b}(\beta - \theta) & \text{if } \beta_a < \theta \le \beta \end{cases} \tag{7}$$

$$f''(\theta) = \begin{cases} \frac{2h}{\beta\beta_a} & \text{if } 0 \le \theta \le \beta_a \\ -\frac{2h}{\beta\beta_b} & \text{if } \beta_a < \theta \le \beta \end{cases} \tag{8}$$

The second piece of parabolic curve will contribute in the chart "$\tan\varphi$ x θ" with a strictly decreasing function, Figure 4, so that this section has minimum and maximum values at the endpoints of its domain. This implies that most of the study should be done in the first parabolic portion. Then, for the first parabolic section, Eq. (5) becomes:

$$\frac{2h}{\beta\beta_a}(\frac{h}{\beta\beta_a}\theta_0^2 + R_p) - (\frac{2h}{\beta\beta_a}\theta_0)^2 = 0$$

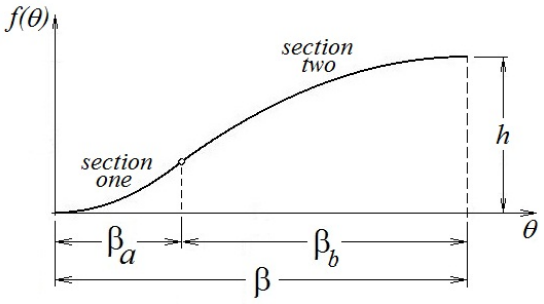

Figure 3. The parabolic curve motion consists of two parabolic sections

what makes immediate:

$$\theta_0 = \sqrt{\beta\beta_a \frac{R_p}{h}} \tag{9}$$

Now, squaring Eq. (4) and inserting Eqs. (6) and (7) result in:

$$\tan^2\hat{\varphi} = \frac{(\frac{2h}{\beta\beta_a})^2\theta_0^2}{(\frac{h}{\beta\beta_a}\theta_0^2 + R_p)^2}$$

From Eq. (9), $\theta_0^2 = \beta\beta_a\frac{R_p}{h}$, which can be inserting in the above expression to get:

$$\tan^2\hat{\varphi} \quad = \quad \frac{h}{\beta\beta_a R_p}$$

which implies that

$$\frac{R_p}{h} = \frac{1}{\beta\beta_a\tan^2\hat{\varphi}} \tag{10}$$

and comparing Eq. (33) with Eq. (9), we conclude that

$$\theta_0 = \frac{1}{\tan\hat{\varphi}} \tag{11}$$

Since this development considered only the first section of the parabolic curve, the result applies only when $\beta_a > \theta_0$, Figure 4b. Furthermore, we can conclude from Eq. (11) that Eq. (10) should apply only if

$$\beta_a > \frac{1}{\tan\hat{\varphi}} \tag{12}$$

For the situation where $\beta_a \leq \frac{1}{\tan\hat{\varphi}}$, Figure 4a, the maximum point θ_0 will occur at β_a and, by replacing this in Eq. (4), will result in

$$\tan\hat{\varphi} = \frac{\frac{2h}{\beta\beta_a}\beta_a}{\frac{h}{\beta\beta_a}\beta_a^2 + R_p}$$

which provides that

$$\frac{R_p}{h} = \frac{2}{\beta\tan\hat{\varphi}} - \frac{\beta_a}{\beta} \tag{13}$$

The final the result for the parabolic curve can be expressed by

$$\frac{R_p}{h} = \begin{cases} \frac{2}{\beta\tan\hat{\varphi}} - \frac{\beta_a}{\beta} & \text{if } \beta_a \leq \frac{1}{\tan\hat{\varphi}} \\ \frac{1}{\beta\beta_a\tan^2\hat{\varphi}} & \text{if } \beta_a > \frac{1}{\tan\hat{\varphi}} \end{cases} \tag{14}$$

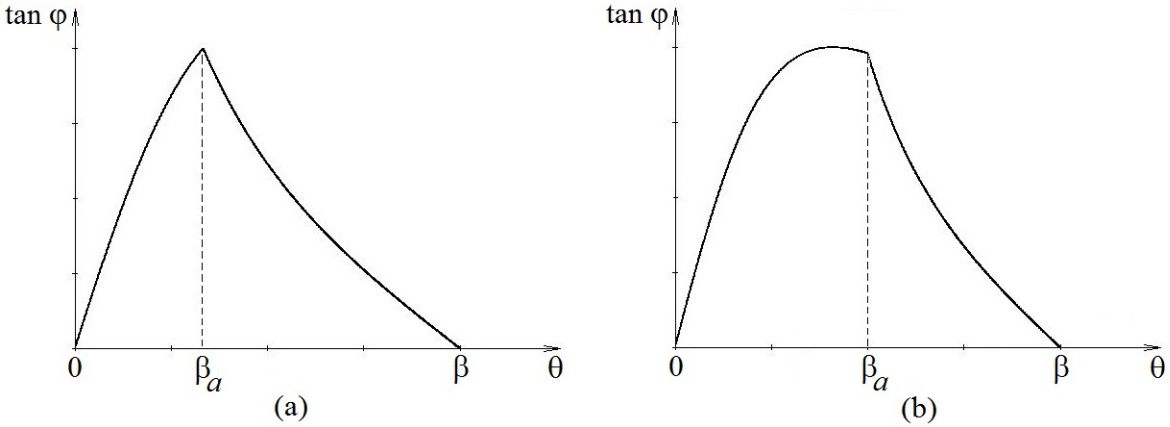

Figure 4. Diagram $\tan\varphi$ x θ for the parabolic curve; in (a) the maximum of $tan\varphi$ occurs at β_a and in (b) the maximum occurs in the interval $]0, \beta_a[$

4.2 Calculation of R_p for the Simple Harmonic Motion

For the simple harmonic motion, the function f and its derivatives take the form

$$f(\theta) = \frac{h}{2}(1 - \cos\frac{\pi}{\beta}\theta) \tag{15}$$

$$f'(\theta) = \frac{h\pi}{2\beta}\sin\frac{\pi}{\beta}\theta \tag{16}$$

$$f''(\theta) = \frac{h\pi^2}{2\beta^2}\cos\frac{\pi}{\beta}\theta \tag{17}$$

In this case, Eq. (5) can be simplified to

$$\cos\frac{\pi}{\beta}\theta_0(1 - \cos\frac{\pi}{\beta}\theta_0 + \frac{2R_p}{h}) - \sin^2\frac{\pi}{\beta}\theta_0 = 0$$

and using the trigonometric identity $\sin^2\frac{\pi}{\beta}\theta_0 = 1 - \cos^2\frac{\pi}{\beta}\theta_0$, one obtains

$$\cos\frac{\pi}{\beta}\theta_0 = \frac{h}{h + 2R_p}$$

Now, squaring the Eq. (4) and inserting the functions $f(\theta_0)$ and $f'(\theta_0)$ result in

$$\tan^2\hat{\varphi} = \frac{\pi^2}{\beta^2}\frac{1 - \cos^2\frac{\pi}{\beta}\theta_0}{(\frac{h+2R_p}{h} - \cos\frac{\pi}{\beta}\theta_0)^2} \tag{18}$$

substituting the expression $\cos\frac{\pi}{\beta}\theta_0 = \frac{h}{h+2R_p}$ in the above equation leads to

$$\tan^2\hat{\varphi} = \frac{\pi^2}{\beta^2}\frac{1}{4\frac{R_p}{h} + 4\frac{R_p^2}{h^2}}$$

which is the same as

$$(\frac{R_p}{h})^2 + \frac{R_p}{h} - \frac{\pi^2}{4\beta^2\tan^2\hat{\varphi}} = 0$$

Since $\frac{R_p}{h} > 0$, the solution of that equation is

$$\frac{R_p}{h} = \frac{1}{2}\sqrt{1 + (\frac{\pi}{\beta\tan\hat{\varphi}})^2} - \frac{1}{2} \tag{19}$$

4.3 Calculation of R_p for the Double Harmonic Motion

For the double harmonic motion the function $f(\theta)$ is

$$f(\theta) = \frac{h}{2}[(1 - \cos\frac{\pi}{\beta}\theta) - \frac{1}{4}(1 - \cos\frac{2\pi}{\beta}\theta)]$$

For convenience, let us replace $\cos\frac{2\pi}{\beta}\theta = \cos^2\frac{\pi}{\beta}\theta - \sin^2\frac{\pi}{\beta}\theta$ in the above equation, obtaining another form and its derivatives:

$$f(\theta) = \frac{h}{4}(1 - (2 - \cos\frac{\pi}{\beta}\theta)\cos\frac{\pi}{\beta}\theta) \tag{20}$$

$$f'(\theta) = \frac{h\pi}{2\beta}(1 - \cos\frac{\pi}{\beta}\theta)\sin\frac{\pi}{\beta}\theta \tag{21}$$

$$f''(\theta) = \frac{h\pi^2}{2\beta^2}(\cos\frac{\pi}{\beta}\theta - 2\cos^2\frac{\pi}{\beta}\theta + 1) \tag{22}$$

For this case Eq. (5), after simplification, will be

$$(\cos\frac{\pi}{\beta}\theta - 1)(\frac{4R_p}{h} + 2\cos\frac{\pi}{\beta}\theta - \cos^2\frac{\pi}{\beta}\theta + 8\frac{R_p}{h}\cos\frac{\pi}{\beta}\theta - 1) = 0$$

since $\theta = 0$ is not a maximum for $\tan\varphi$, the conclusion is that

$$\cos^2\frac{\pi}{\beta}\theta + (2 + 8\frac{R_p}{h})\cos\frac{\pi}{\beta}\theta - (1 - \frac{4R_p}{h}) = 0$$

and, since $\cos\frac{\pi}{\beta}\theta \leq 1$ and $\frac{R_p}{h} > 0$, the positive sign of the radical can be ignored, obtaining for solution

$$\cos\frac{\pi}{\beta}\theta = 1 + 4\frac{R_p}{h} - 2\frac{R_p}{h}\sqrt{1 + \frac{3h}{4R_p}} \tag{23}$$

Now, squaring the Eq. (4) and inserting $f(\theta_0)$ and $f'(\theta_0)$ one obtains

$$\tan^2\hat{\varphi} = \frac{4\pi^2}{\beta^2}\frac{(1 - \cos^2\frac{\pi}{\beta}\theta_0)(1 - \cos\frac{\pi}{\beta}\theta_0)^2}{[1 - (2 - \cos\frac{\pi}{\beta}\theta_0)\cos\frac{\pi}{\beta}\theta_0 + 4\frac{R_p}{h}]^2}$$

Substituting Eq. (23) in the expression above and defining a K factor as

$$K = \sqrt{1 + 3(\frac{\pi}{\beta\tan^2\hat{\varphi}})^2} \tag{24}$$

results in the following solution for $\frac{R_p}{h}$

$$\frac{R_p}{h} = \frac{3(K-1)^2}{8K - 4} \tag{25}$$

4.4 Calculation of R_p for the Cycloidal Motion

For the cycloidal motion, the function $f(\theta)$ and its derivatives have the form:

$$f(\theta) = h(\frac{\theta}{\beta} - \frac{1}{2\pi}\sin\frac{2\pi}{\beta}\theta) \tag{26}$$

$$f'(\theta) = \frac{h}{\beta}(1 - \cos\frac{2\pi}{\beta}\theta) \tag{27}$$

$$f''(\theta) = \frac{2\pi h}{\beta^2}\sin\frac{2\pi}{\beta}\theta \tag{28}$$

It is more convenient to use the Eq. (3) and, by substituting Eq. (27) and Eq. (28) in it, one obtains

$$\tan\hat{\varphi} = \frac{2\pi}{\beta}\frac{\sin\frac{2\pi}{\beta}\theta_0}{1 - \cos\frac{2\pi}{\beta}\theta_0}$$

Using the trigonometric identities, $\sin\frac{2\pi}{\beta}\theta_0 = 2\sin\frac{\pi}{\beta}\theta_0\cos\frac{\pi}{\beta}\theta_0$ and $\cos\frac{2\pi}{\beta}\theta_0 = \cos^2\frac{\pi}{\beta}\theta_0 - \sin^2\frac{\pi}{\beta}\theta_0$ results in

$$\tan\hat{\varphi} = \frac{2\pi}{\beta}\frac{1}{\tan\frac{\pi}{\beta}\theta_0}$$

which leads to

$$\tan\frac{\pi}{\beta}\theta_0 = \frac{2\pi}{\beta}\frac{1}{\tan\hat{\varphi}} \tag{29}$$

Now, using Eq. (4) with equations (26) and (27) and replacing θ by θ_0 result in

$$\tan\hat{\varphi} = \frac{\frac{h}{\beta}(1-\cos\frac{2\pi}{\beta}\theta_0)}{h(\frac{\theta}{\beta} - \frac{1}{2\pi}\sin\frac{2\pi}{\beta}\theta_0) + R_p}$$

which provides:

$$\frac{R_p}{h} = \frac{1}{2\pi}\sin\frac{2\pi}{\beta}\theta_0 + \frac{1-\cos\frac{2\pi}{\beta}\theta_0}{\beta\tan\hat{\varphi}} - \frac{\theta_0}{\beta}$$

Now, using the two trigonometric relations for double angles in sin and cos, one can get

$$\frac{R_p}{h} = \frac{1}{2\pi}(\frac{2\tan\frac{\pi}{\beta}\theta_0}{1+\tan^2\frac{\pi}{\beta}\theta_0}) + \frac{1-(\frac{1-\tan^2\frac{\pi}{\beta}\theta_0}{1+\tan^2\frac{\pi}{\beta}\theta_0})}{\beta\tan\hat{\varphi}} - \frac{\theta_0}{\beta}$$

using Eq. (29) in the above equation we reach

$$\frac{R_p}{h} = \frac{2}{\beta\tan\hat{\varphi}} - \frac{\theta_0}{\beta}$$

Noting that $\frac{\theta_0}{\beta} = \frac{1}{\pi}\arctan(\frac{2\pi}{\beta\tan\hat{\varphi}})$, Eq. (29), the above equation result in

$$\frac{R_p}{h} = \frac{1}{\pi}\left(\frac{2\pi}{\beta\tan\hat{\varphi}} - \arctan(\frac{2\pi}{\beta\tan\hat{\varphi}})\right) \tag{30}$$

4.5 Offset Cam Followers

Offset cam followers are only used when the analysis of the radial follower has shown that the cam behaviour was unsatisfactory. The analyst should be especially careful, because in this type of cam follower, the pressure angle decreases on the rise, but increases in the same proportion on the return.

For this case the process of obtaining the equations is similar to the previous case and one should be just careful to properly introduce the equations (1) and (2), which contain the ϵ term, and Eq. (3).

After proceeding with this development, one will find the following expressions,

The final results are for the Parabolic Motion

$$R_p = \begin{cases} \sqrt{\varepsilon^2 + \left[\frac{2h-\varepsilon\beta}{\beta\tan\hat{\varphi}} - \frac{h\beta_a}{\beta}\right]^2} & \text{if } \beta_a \leq \frac{1}{\tan\hat{\varphi}} \\ \sqrt{\varepsilon^2 + \left[\frac{h}{\beta\beta_a\tan^2\hat{\varphi}} - \frac{\varepsilon}{\tan\hat{\varphi}}\right]^2} & \text{if } \beta_a > \frac{1}{\tan\hat{\varphi}} \end{cases} \tag{31}$$

for the Simple Harmonic Motion

$$R_p = h\sqrt{(\frac{\varepsilon}{h})^2 + \left[\frac{1}{2}\sqrt{1+(\frac{\pi}{\beta\tan\hat{\varphi}})^2} - \frac{\varepsilon}{h\tan\hat{\varphi}} - \frac{1}{2}\right]^2} \tag{32}$$

and for the Cycloidal Motion

$$R_p = h\sqrt{(\frac{\varepsilon}{h})^2 + \left[\frac{2h-\varepsilon\beta}{\beta h\tan\hat{\varphi}} - \frac{1}{\pi}\arctan(\frac{2\pi}{\beta\tan\hat{\varphi}})\right]^2} \tag{33}$$

In this case, the expressions for θ_0, though they may be obtained, are very complex and are of little interest.

4.6 Numerical Methods

If we have R_p, the solution of Eq. (5) can be easily obtained analytically, this makes it easy to obtain a numerical algorithm, since we can test the values of φ comparing them to $\hat{\varphi}$ for a given set of related R_p's conveniently chosen as below.

error $\leftarrow 0.0001$
$\hat{\varphi} \leftarrow$ data input
$\Delta R_p \leftarrow 0.001$
$R_p \leftarrow 0.0$
While ($\tan\varphi - \tan\hat{\varphi} >$ error) **then**
  $\theta_0 \leftarrow$ solution of $[f''(\theta)(f(\theta)+R_p) - f'(\theta)^2 = 0]$
  $\tan\varphi \leftarrow f'(\theta_0)/(f(\theta_0)+R_p)$
  $R_p \leftarrow R_p + \Delta R_p$
EndWhile
data out $\leftarrow R_p$

4.7 Summary of Expressions

The Tab. 1 compiles all results in a single table, while also allowing a comparison between the four types of equations.

Table 1. Summary of Results.

Curve	θ_0	K	$\frac{R_p}{h}$
Harmonic	$\frac{\beta}{\pi}\arccos\frac{h}{h+2R_p}$	$\sqrt{1+(\frac{\pi}{\beta\tan\hat{\varphi}})^2}$	$\frac{K-1}{2}$
Double Harmonic	$\frac{\beta}{\pi}\arccos(1+4\frac{R_p}{h}-2\frac{R_p}{h}\sqrt{1+\frac{3h}{4R_p}})$	$\sqrt{1+3(\frac{\pi}{\beta\tan^2\hat{\varphi}})^2}$	$\frac{3(K-1)^2}{8K-4}$
Cycloid	$\frac{\beta}{\pi}\arctan\frac{2\pi}{\beta\tan\hat{\varphi}}$	$\frac{2\pi}{\beta\tan\hat{\varphi}}$	$\frac{1}{\pi}(K-\arctan K)$
Parabolic $\beta_a \leq \frac{1}{\tan\hat{\varphi}}$	$\sqrt{\beta\beta_a\frac{R_p}{h}}$	$\frac{1}{\beta\tan\hat{\varphi}}$	$2K-\frac{\beta_a}{\beta}$
or $\beta_a > \frac{1}{\tan\hat{\varphi}}$	β_a	$\frac{1}{\beta\tan\hat{\varphi}}$	$\frac{\beta}{\beta_a}K^2$

5. RESULT ANALYSIS

In this section a comparison between results obtained by a traditional numerical method with results obtained by using the analytical functions developed in this work. That comparison can be seen in Figs. 5 and 6. In these graphs an analysis

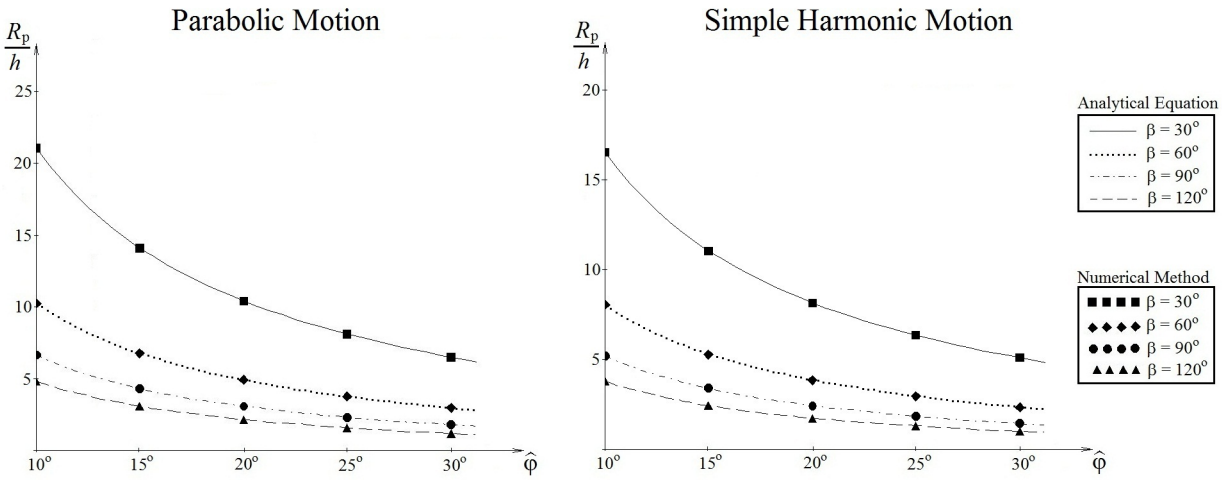

Figure 5. Application of a numerical method and correspondent analytical equations for Parabolic and Harmonic motions

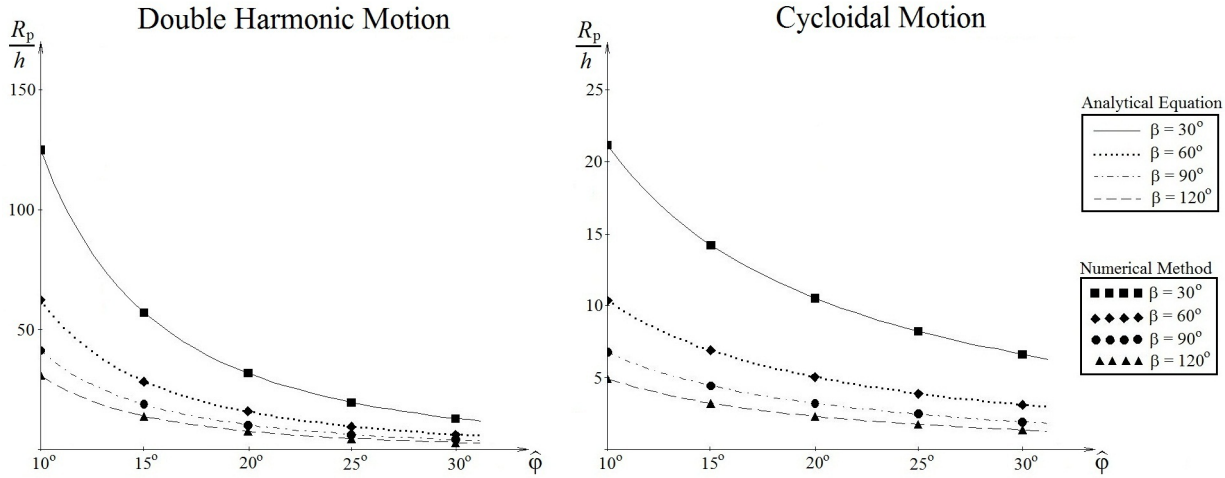

Figure 6. Application of a numerical method and correspondent analytical equations for Double Harmonic and Cycloidal motions

was made for four elevation angles, $\beta = 30^o$, $\beta = 60^o$, $\beta = 90^o$ and $\beta = 120^o$ and considering the maximum pressure angle $\hat{\varphi}$ ranging from 10^o to 30^o. The curves resulting from the analytical equations are continuous, but for the numerical method the results were taken only for values of maximum pressure angle of 10^o, 15^o, 20^o, 25^o and 30^o. For the numerical method we use the algorithm presented in section 4.6, coded in C++ language, conveniently replacing the function $f(\theta)$ and its derivatives for each curve type.

6. REFERENCES

Carra, S., Garziera, R. and Pellegrini, M., 2004. "Synthesis of cams with negative radius follower and evaluation of the pressure angles". *Mechanism and Machine Theory*, Vol. 34, pp. 1017–1032.

Chen, F.Y., 1982. "Mechanics and design of cam mechanisms". *Pergamon Press*, pp. 155–162.

Gonzales-Palacios, M.A. and Angeles, J., 1993. *Cam Synthesis*. Kluwer Academic Publishers, The Netherlands.

Jesen, P.W., 1987. *Cam Design and Manufacture*. New York and Base.

Koomok, M. and Muffley, R.V., 1955. *Plate cam design pressure angle analysis*. New York.

Norton, R.L., 2009. *Cam Design and Manufacturing Handbook*. Industrial Press Inc, New York.

Rothbart, H.A., 2004. *Cam design handbook*. McGraw-Hill Professional, New York.

Uicker, J.J., Pennock, G. and Shigley, J.E., 2010. *Theory of Machines and Mechanisms*. Oxford University Press, USA.

Yu, Q. and Lee, H.P., 1998. "Size optimization of cam mechanisms with translating roller followers". *Journal of Mechanical Engineering Science*, Vol. 212, No. 5, pp. 381–386.

7. Responsibility notice

The authors are the only responsible for the printed material included in this paper